ISSN 1674-1056
http://cpb.iphy.ac.cn
http://iopscience.iop.org/cpb
中国物理 B
Chinese Physics
中国物理 Chinese Physics B

Ignition characteristics of pre-combustion plasma jet igniter

Si-Bo Wang(王思博)[1], Jin-Lu Yu(于锦禄)[1], Jing-Feng Ye(叶景峰)[2], Guo-Hua Li(李国华)[2], Zhao Chen(陈朝)[1], Lu-Yun Jiang(蒋陆昀)[1], Chen-Li Gu(古晨力)[3]

Citation: Chin. Phys. B . 2019, 28(11): 114702 . **doi:** 10.1088/1674-1056/ab470e
Journal homepage: http://cpb.iphy.ac.cn; http://iopscience.iop.org/cpb

What follows is a list of articles you may be interested in

Shock oscillation in highly underexpanded jets

Xiao-Peng Li(李晓鹏), Rui Zhou(周蕊), Xiao-Ping Chen(陈小平), Xue-Jun Fan(范学军), Guo-Shan Xie(谢国山)
Chin. Phys. B . 2018, 27(9): 094705 . **doi:** 10.1088/1674-1056/27/9/094705

Numerical investigation of the interaction of the turbulent dual-jet and acoustic propagation

Yi-Ming Li(李一明), Bao-Kuan Li(李宝宽), Feng-Sheng Qi(齐凤升), Xi-Chun Wang(王喜春)
Chin. Phys. B . 2017, 26(2): 024701 . **doi:** 10.1088/1674-1056/26/2/024701

Laser-induced breakdown spectroscopy applied to the characterization of rock by support vector machine combined with principal component analysis

Hong-Xing Yang(杨洪星), Hong-Bo Fu(付洪波), Hua-Dong Wang(王华东), Jun-Wei Jia(贾军伟), Markus W Sigrist, Feng-Zhong Dong(董凤忠)
Chin. Phys. B . 2016, 25(6): 065201 . **doi:** 10.1088/1674-1056/25/6/065201

Effect of noncircular orifice plates on the near flow field of turbulent free jets

Xu Min-Yi, Tong Xing-Qing, Yue Dan-Ting, Zhang Jian-Peng, Mi Jian-Chun, Nathan G. J., Kalt P. A. M.
Chin. Phys. B . 2014, 23(12): 124703 . **doi:** 10.1088/1674-1056/23/12/124703

Mean and fluctuating velocity fields of a diamond turbulent jet

Xu Min-Yi, Zhang Jian-Peng, Mi Jian-Chun, Nathan G. J., Kalt P. A. M.
Chin. Phys. B . 2013, 22(3): 034701 . **doi:** 10.1088/1674-1056/22/3/034701

Ignition characteristics of pre-combustion plasma jet igniter*

Si-Bo Wang(王思博)[1], Jin-Lu Yu(于锦禄)[1,†], Jing-Feng Ye(叶景峰)[2], Guo-Hua Li(李国华)[2], Zhao Chen(陈朝)[1], Lu-Yun Jiang(蒋陆昀)[1], and Chen-Li Gu(古晨力)[3]

[1] *Air Force Engineering University, Xi'an* 710038, *China*
[2] *State Key Laboratory of Laser Interaction with Matter, Northwest Institute of Nuclear Technology, Xi'an* 710038, *China*
[3] *The University of Sheffield, Western Bank Sheffield, S*10 2*TN, UK*

(Received 26 July 2019; revised manuscript received 23 September 2019; published online 30 October 2019)

At present, aero-engines face a major need to widen the ignition envelope. In order to provide a technical support to expand the high altitude ignition envelope of aero-engines, in this article we propose a novel ignition technology, *i.e.*, "pre-combustion plasma jet ignition technology". In this paper, we also design a pre-combustion plasma jet igniter. Its discharge characteristics, jet characteristics, and ignition effects are studied. The results show that increasing the equivalent ratio of jet gas can enhance the discharge stability and increase the duty cycle. At the same time, it can reduce working power and energy consumption. The increase of equivalent ratio in jet gas can enhance the length and ignition area of plasma jet. In the process of ignition, the pre-combustion plasma jet igniter has obvious advantages, suchn as shortening the ignition delay time and enlarging the ignition boundary. When the airflow velocity is 39.11 m/s and the inlet air temperature is 80 °C, compared with the spark igniter and the air plasma jet igniter, the pre-combustion plasma jet igniter has an ignition boundary that is expanded by 319.8% and 55.7% respectively.

Keywords: pre-combustion, discharge stability, ignition delay time, ignition boundary

PACS: 47.27.wg, 52.25.Kn, 52.25.Jm, 52.50.Nr **DOI:** 10.1088/1674-1056/ab470e

1. Introduction

Plasma is a form of material composed of free electrons and charged ions. It is widely found in the universe and is often considered as the fourth state of matter. When the temperature of ordinary gas increases, the thermal motion of gas particles intensifies and strong collisions happen between particles, and as a result a large number of electrons in atoms or molecules are knocked off. This highly ionized, macroscopically electroneutral gas is called plasma.[1–3] Plasma ignition is a process in which the gas discharge forms a high-temperature region and stimulates a large number of active particles to ignite the combustible mixture rapidly.[4,5] Studies have shown that the mechanism of plasma ignition is mainly manifested in three effects:[6,7] thermal effect, chemical effect, and aerodynamic effect.[8,9] Plasma, flow, heat, and mass transfer are highly coupled.[10]

Ju *et al.*[11,12] and Mao *et al.*[13] focused on studying the application of plasma-assisted combustion technology and the combustion mechanism. Dresven *et al.*[14] and Pfender *et al.*[15,16] studied the structure and turbulence characteristics of the plasma jet. Bozhenkov *et al.*[17] developed a numerical model for studying high-voltage nanosecond-pulse discharge ignition. Yu *et al.*[18,19] used the plasma jet igniter and the spark plug to ignite the propane/air mixture respectively. It was found that the plasma ignition can significantly prolong the ignition limit and shorten the ignition delay time. The applications of plasma in ignition and combustion-supporting field have also been investigated. Watanabe *et al.*[20] conducted an experiment on the cathode of an inductively coupled plasma exciter, pointing out that neutral particle concentration and pressure have a significant influence on plasma ignition. Most plasma jet igniters studied before took air as a discharge medium.[21] Compared with traditional spark igniter, the plasma jet igniter has obvious advantages in the ignition. Therefore, in this paper we present our designed pre-combustion plasma jet igniter. During ignition, it can form a high-temperature arc mixed with methane flame jet, which has a longer ignition jet, larger ignition area, and higher ignition temperature. It is found that the pre-combustion plasma jet igniter has obvious advantages over the former air plasma jet igniter. Therefore, this paper focuses on the study of the working characteristics of this type of pre-combustion plasma jet igniter.

In this paper, the discharge characteristics and jet characteristics of a pre-combustion plasma jet igniter are studied. At the same time, the ignition experiment is carried out on the combustion chamber of a certain type of aero-engine. The ignition characteristics of the pre-combustion plasma jet igniter are compared with those of the traditional spark igniter and air plasma jet igniter. The ignition delay time and ignition boundary are explored.

*Project supported by the National Natural Science Foundation of China (Grant Nos. 51776223 and 91741112).
†Corresponding author. E-mail: yujinlu1@163.com
© 2019 Chinese Physical Society and IOP Publishing Ltd

2. Experimental system

2.1. Pre-combustion plasma igniter design

The pre-combustion plasma igniter is a novel type of igniter that is different from the existing plasma igniters. Figure 1 shows the schematic diagram of the pre-combustion plasma igniter designed in this paper. The igniter is mainly composed of outer casing, air inlet, fuel passage, cathode, anode, cyclone and insulation parts. The fuel passage is located in the center of the cathode and is made of a ceramic tube with a diameter of 0.4 mm. The insulating member and the cyclone are made of polytetrafluoroethylene (PTFE) with good mechanical properties and certain temperature resistance. The anode and cathode are made of tungsten-copper alloy with good electrical conductivity and high-temperature resistance.

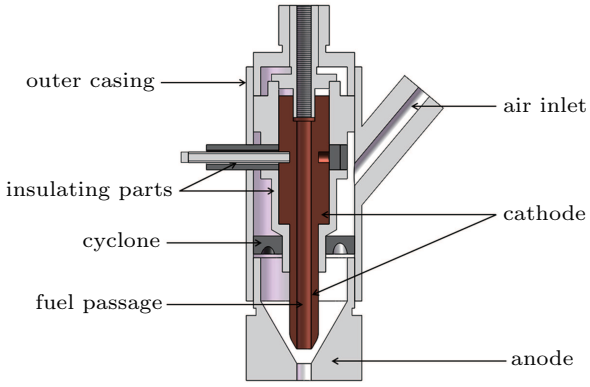


Fig. 1. Pre-combustion plasma jet igniter.

The structure of the annular tube cathode combined with the cyclone is designed. When igniter works, air flows into igniter from the air inlet on the sidewall of the igniter. And the swirling gas is generated through the cyclone so that the arc rotates and slides on the annular cathode head. It reduces the ablation of the electrode. At the same time, methane is ejected from the fuel passage into the cathode copper tube, which is premixed with the swirling gas, and ionized in the ionization region. And then it forms a high energy plasma jet at the anode exit, igniting the combustible mixture in the combustion chamber of the engine.

This type of pre-combustion plasma jet igniter is sprayed with methane near the exit of a conventional plasma igniter and the methane blended with a high-temperature plasma jet in a small area near the outlet. The methane is ignited by high-temperature arc while being ionized, forming a high speed and a wide range plasma jet. The jet is a swirling plasma jet with high-temperature and high-speed. When it is injected into the combustion chamber, under the combined action of centrifugal force and inertial force, the jet exchanges momentum, heat and mass with the surrounding medium and quickly ignites the combustible mixture in the combustion chamber. Compared with the conventional plasma ignition technology, the pre-combustion plasma jet ignition has a pre-combustion process of the fuel, which releases a large amount of heat. Its advantages include enhancing the ignition energy, expanding the ignition area, strengthening the jet stiffness, and reducing the energy consumption of the igniter. Simultaneously the pre-combustion plasma jet ignition improves the reliability and success rate of ignition and provides a feasible solution for the specific application of plasma ignition on aero-engine.

2.2. Experimental system

The experimental system of the pre-combustion plasma jet igniter's working characteristic is shown in Fig. 2. The experimental system consists of a plasma jet igniter, a plasma power, a gas supply system, an oscilloscope, a current-voltage probe, a high-speed charge-coupled device (CCD) camera, and an OH–PLIF experimental system. The plasma power is a high-frequency and high-voltage pulse starting arc with a voltage of 3 kV and a 24-V DC stabilized arc power. Two D08-1F flow meters and flow regulators are used to control the gas flow of methane and air respectively. The sampling rate of the Tektronix 4104B oscilloscope is 1 GB/s, and the Tektronix P6015A high voltage probe is used for detecting the voltage signal. The Tektronix TCP0030 AC/DC current probe is used to measure the current signal. The high-speed CCD camera has a maximum sampling frequency of 682222 ftps and a minimum exposure time of 1 μs. The high-speed CCD camera and the intensified charge-coupled device (ICCD) cameras capture the pre-combustion plasma jet at the same position. So the shape of the jet and the arc can be better captured and compared with the captured OH–PLIF image. The Canon digital camera is used to record the shape of the plasma jet's intuitive flame. The DG625 signal generator is used to control the timing of the experimental system. The laser used in the OH–PLIF experimental system is generated by a YAG laser + tunable dye laser + frequency multiplier. The wavelength of the laser is 285.004 nm, and the pulse width is about 8 ns. The single pulse energy is about 7 mJ. After the laser beam is shaped by the cylindrical microlens array and the convex lens, a laser chip having a width of 50 mm and a thickness of 0.2 mm is formed in the measurement area. The ICCD camera is placed in a direction perpendicular to the light film. The camera resolution is 1024×1024 pixels, the door switch is turned on for 20 ns, and a (320±20)-nm narrow bandpass filter is placed in front of the camera lens to filter out stray light.

The experimental system of the pre-combustion plasma jet igniter's ignition characteristic is shown in Fig. 3. The experimental system consists of three parts: the gas supply system, the working system, and the measurement system. The gas supply system is divided into two parts, one is a gas supply

system of the main gas path and the other is a gas supply system of the plasma igniter. The main air supply system consists of an air compressor, a gas storage tank, a frozen compressed air dryer (FCAD), and a heater. The air supply source of the igniter is two bottles of high-pressure gas, and the flow rate is controlled by the flow meter. The measurement system consists of an acquisition computer, a high-speed CCD camera, two photomultiplier tubes that capture O and CH signals respectively. The working system consists of an igniter, a plasma power, a fuel supply system, and the experimental section of a certain aero-engine combustion chamber. The structural diagram of the experimental section of the combustion chamber and the installation position of the igniter are shown in Fig. 4. The area A and the area B in Fig. 4 indicate the mounting positions of the photomultiplier (O) and the photomultiplier (CH), respectively.

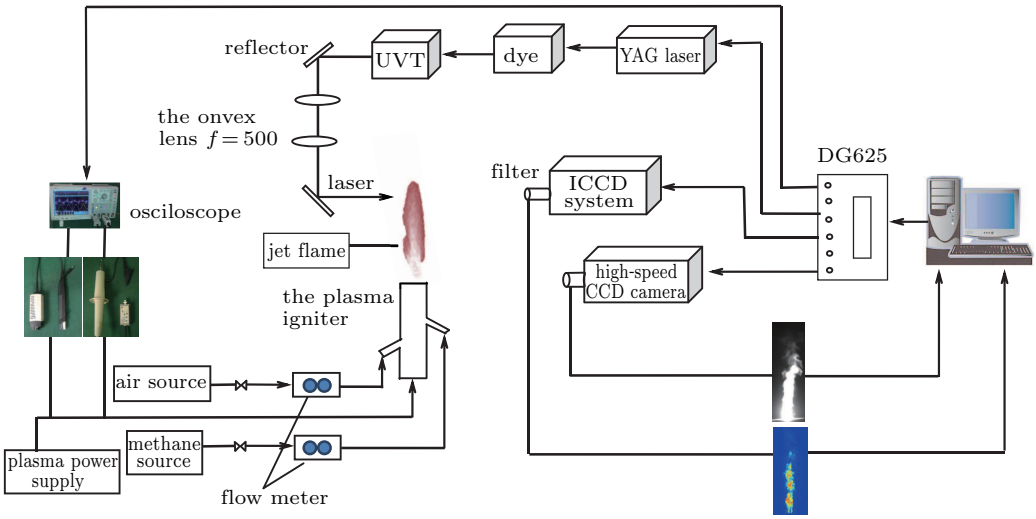


Fig. 2. Working characteristics of experimental system for pre-combustion plasma jet igniter.

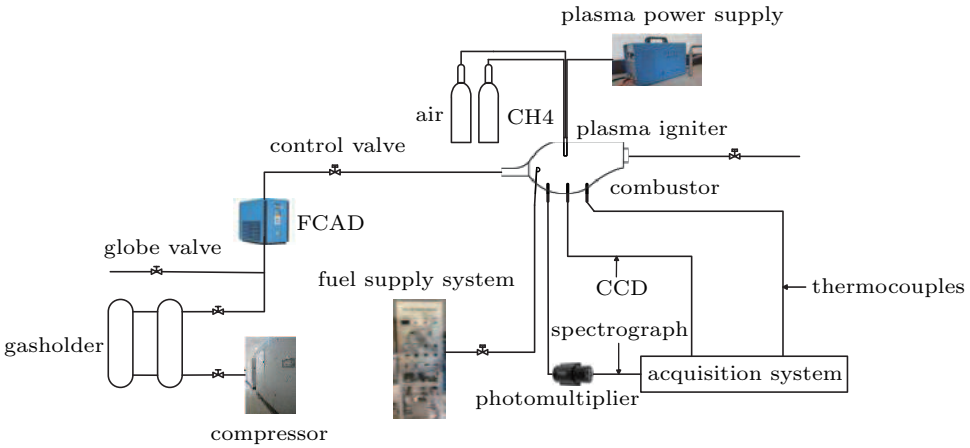


Fig. 3. Schematic diagram of ignition experimental system.

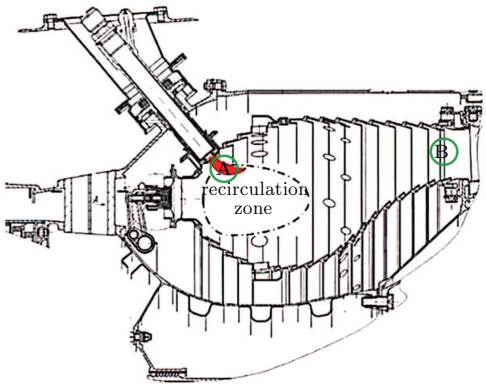


Fig. 4. Schematic diagram of combustion chamber structure.

3. Results and discussion

3.1. Discharge characteristics of pre-combustion plasma jet igniter

Discharge characteristic is one of the most important characteristics of plasma igniter, which can reflect the characteristics of igniter operating stability, voltage, and current changes. In this subsection, the influence of the equivalent ratio of discharge medium on the discharge characteristic is studied, which lays a foundation for the study of ignition characteristics.

Both the reaction of ionization and combustion take place

in the pre-combustion plasma jet. So the pre-combustion plasma jet shows the characteristic of the plasma and the flame. When the pre-combustion plasma jet igniter is working, the discharge process can be divided into three stages: the accumulated voltage stage, breakdown stage, and stable arc stage. Figure 5 presents a schematic diagram showing current and voltage waveforms obtained when the input current is 25 A. (i) Accumulated voltage stage: Before the breakdown occurs, the discharge is in the accumulated voltage stage. At this time, the current is 0 and no breakdown happens. And the voltage fluctuates within a certain interval. Longer accumulated voltage stage time is not conducive to plasma jet continuity and stability. (ii) Breakdown stage: After the voltage reaches a certain value, it enters into the breakdown stage. The discharge medium is broken down to form a discharge path. (iii) Stable arc stage: After the discharge medium is broken down, a discharge path formed. So a relatively stable discharge region is formed. Now the resistance is greatly reduced; the voltage is rapidly reduced; the current is increased. The current and voltage become stable. It enters into the stable arc stage.

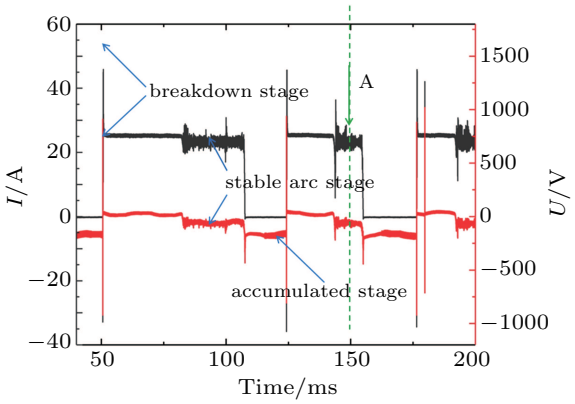


Fig. 5. The schematic diagram of discharge characteristics of the pre-combustion plasma jet igniter.

The characteristics of the time and period of the steady arc phase during the operation of the igniter directly reflect the stability of the discharge. In order to better describe the discharge stability, the average arc stability time T_{as} and the average duty cycle Da are defined as $T_{as} = T_s/n$ and $D_a = T_s$, respectively, where T_s is the total time of the steady arc stage of the sampling segment, n is the total number of breakdowns of the sampling segment, and T is the total time of the sampling segment. The total jet gas flow rate is kept at 60 L/min, the input current is 25 A, and the sampling time is 200 ms. By changing the equivalence ratio of the jet gas, the average arc stability time and the average duty cycle vary with the equivalence ratio as shown in Fig. 6.

As can be seen from Fig. 6, with equivalence ratio increasing, the average arc stability time and duty cycle increase. When the equivalence ratio increases from 0 to 0.5, the average arc stability time and duty cycle increase greatly. When the equivalent ratio is 0.5, the average arc stability time is twice as long as that at $\varphi = 0$, and the duty cycle is three times more than that at $\varphi = 0$. As the equivalence ratio continues to increase, the increase is tapering off. This is due mainly to the fact that as the equivalent ratio increases, a large number of active particles produced by the combustion of methane are more favorable for the formation of discharge channels, which makes the arc not easily blown off by the jet gas. Even if it is blown off, it can be broken down quickly again, so the discharge stability is improved.

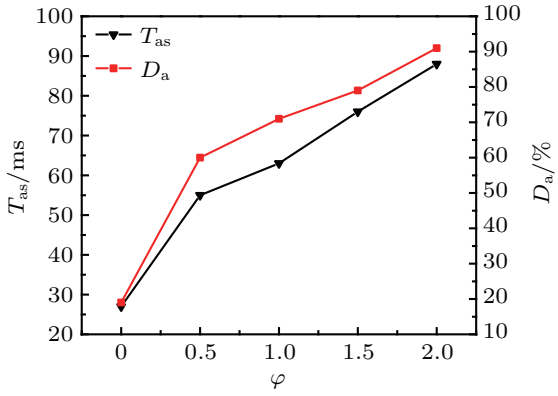


Fig. 6. Average time of steady arc stage and duty cycle changing with equivalence ratio.

The breakdown stage is short and has little effect on total working power. During the accumulated voltage stage, I is 0, at which time the working power is 0. In this paper, stable arc stage power is selected as the working power. The total jet gas flow is kept at 60 L/min, and the input current is 25 A. With changing the equivalent ratio of the jet gas, working power changes with φ in the 5S as shown in Fig. 7.

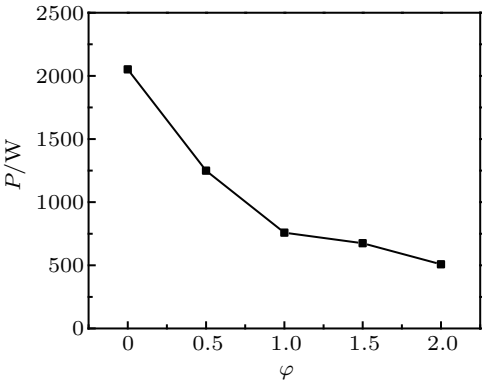


Fig. 7. Power supply changing with equivalent ratio.

As can be seen from Fig. 7, as the equivalent ratio increases, the working power gradually decreases. When the equivalent ratio is 2, the average working power is 507.9 W. When the equivalence ratio is 0, the average working power is 2051.4 W. When the equivalent ratio is 2, compared with that at $\varphi = 0$, average working power is reduced by 75.2%.

This is mainly due to the fact that the working power is greatly affected by the jet gas of this type. When air is used as the jet gas, the components are mainly O_2 molecules and N_2 molecules. Ionization molecules need to break the chemical bonds inside the molecule. However, the energy required to break C–H in methane molecule is less than that needed to break O=O in the O_2 molecule and N≡N in the N_2 molecule. After the addition of methane, the reaction like $N_2(ap)+CH_4 \rightarrow N_2+CH_3+H$ and $N_2(B3)+CH_4 \rightarrow N_2+CH_3+H$ is easier to carry out in the discharge process.[22] This causes the concentration of active particles to increase greatly. At the same time, the chemical energy released during the combustion of methane can also promote the breaking of chemical bonds. Methane combustion produces a large number of active particles, which is also conducive to the formation of the discharge path. So the working power is reduced. Therefore, an increase in the equivalence ratio reduces the working power and thus saves the energy.

3.2. Jet characteristics of pre-combustion plasma jet igniter

Figure 8 shows a schematic diagram of the jet structure of a pre-combustion plasma jet igniter. Figure 8(a) shows the plasma jet flame picture taken by the Canon camera. Figure 8(b) shows the OH distribution image obtained by the OH–PLIF experimental system. Figure 8(c) displays the arc picture taken by the high-speed CCD camera at high exposure time and frequency. As can be seen from Fig. 8(a), the center of the plasma jet is a high-brightness area, which is bright white. In the combustion reaction, the concentration of OH can better reflect the intensity of the reaction. Comparing Fig. 8(b) with Fig. 8(c), it can be seen that the OH intensity in the arc region of the jet is relatively high, so the arc can be observed in the OH distribution image. In the upper part of the arc region, the relative strength of OH decreases, but it is still the core of the reaction. By comparing Figs. 8(a), 8(b), and 8(c), it can be found that the overall structure of the pre-combustion plasma jet is as follows: the bottom is the arc, the middle is the core reaction region, and the periphery is the outer flame region.

Figure 9 shows a schematic diagram displaying the change of the OH distribution pattern of the pre-combustion plasma jet with the equivalent ratio. The pictures show the morphology of the pre-combustion plasma jet taken by the OH–PLIF experiment system changing with equivalent ratio. As can be seen from Figs. 8 and 9, the flame exhibits typical turbulent combustion characteristics such as wrinkles, curls, etc., and is a typical turbulent flame. After the jet gas passes through the cyclone, the rotating jet exits from the nozzle and enters into the large space. During the discharge and combustion, a great deal of heat is released, so the density of the surrounding gas decreases, forming a longitudinal density gradient. In the process of the high-temperature flammable gas diffusing into the surrounding air, the cold and hot gas meet together. Under the combined action of the aerodynamic force and density gradient of the jet gas, the jet flame is more likely to produce folds and form a vortex structure. Besides, the arc shape at the exit of the igniter exhibits a different shape under the combined action of aerodynamic forces and electromagnetic forces.

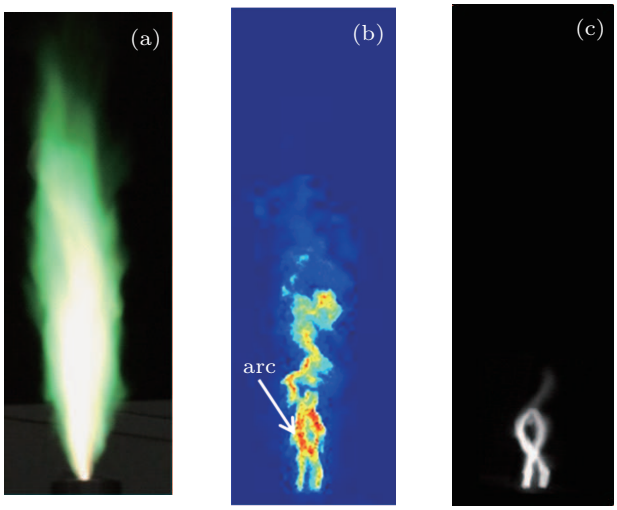


Fig. 8. Pre-combustion plasma jet image taken by (a) Canon camera and (b) OH–PLIF experimental system, and (c) arc image taken by high-speed CCD camera.

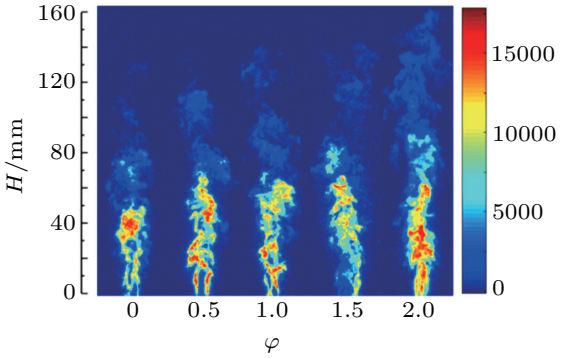


Fig. 9. Schematic diagram of pre-combustion plasma jet configuration changing with equivalent ratio.

The area where the relative strength of the OH signal is greater than 3000 is defined as the core area of the jet. The values of jet height H and the jet core area S of different equivalence ratios are calculated, and 80 sets of data are averaged for each working condition. The results are shown in Fig. 10. It can be seen from the figure that as the equivalence ratio increases, the jet height and the area of the jet core region gradually increase. That is to say, as the equivalent ratio of the jet gas increases, the pre-combustion plasma jet has a stronger penetration capability and a larger ignition area. When the equivalence ratio is 2, the area of the core area of the jet is 2.56 times and the length of the jet is 1.72 times the values of their counterparts in the case of $\varphi = 0$.

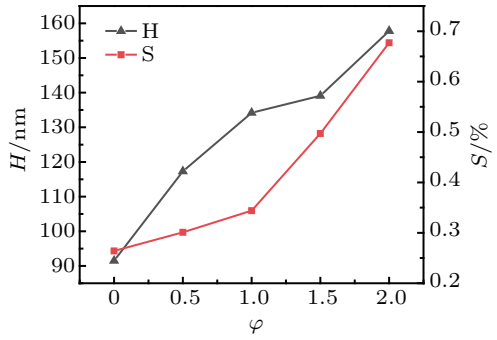


Fig. 10. Average height and average area of pre-combustion plasma jet changing with equivalent ratio.

During the reaction, the main generation routes of OH are $H+O_2=O+OH$ and $HO_2(a^1\Delta g)\rightarrow OH+O$. They occupy a ratio of 80% and 16% respectively. The other paths to generate the OH are $H+HO_2=2OH$, $H_2O+O_2\,(a^1\Delta g)\rightarrow OH+HO_2$, *etc.* The main consumption pathway of OH is $OH+O\rightarrow O_2\,(a^1\Delta g)+H$. It occupies a ratio of 98%. The other paths to consume the OH are the following $OH+HO_2=O_2+H_2O$, $H_2O+O_2=OH+HO_2$, $H+OH=O+H_2$, *etc.*[23]

3.3. Ignition characteristics of pre-combustion plasma jet igniter

3.3.1. Analysis of the ignition process

The ignition process of an aero-engine is divided into three stages: the flame kernel formation stage, the flame propagation stage, and the flame stabilization stage. In order to explore the advantages of pre-combustion plasma jet igniter, the ignition process of spark igniter, air plasma jet igniter, and pre-combustion plasma jet igniter are compared and studied. The inlet gas flow rate of the combustion chamber is 400 m^3/h, that is, the velocity is 31 m/s. The inlet flow temperature is 80 °C. The oil flow rate is 0.285 L/min. So the equivalent ratio is 0.39. In this paper, the high-speed CCD camera is used to capture the whole process of the igniter from the flame kernel formation stage to the flame stabilization stage. The camera exposure time is 10 μs. The camera frame rate is 3×10^4 fps, and the resolution is 768×480. The 0 moment in this paper is set to be the trigger moment of the high-speed CCD camera. The voltage rising edge of the oscilloscope triggers the high-speed CCD camera, and the trigger voltage is set to be 5 V. When the igniter breaks down, the voltage rapidly increases, triggering the high-speed CCD camera to start shooting. The 0 moments on the time axis in Figs. 13 and 15 are the times at which the igniter breaks down.

Figure 11 shows the ignition process of the spark igniter. It can be seen from the figure that the spark ignition produces a small flame kernel and a high-temperature region, in which the fuel–air mixture is ignited. And the flame propagates from the igniter outlet position to the entire combustion chamber. At 2 ms, the flame kernel is generated. In the time interval from 2 ms to 42 ms, the process of expanding the initial flame kernel takes place. At 42 ms, the combustion chamber head is basically ignited. Then the flame continues to propagate backward, and the entire combustion chamber is substantially ignited at 54 ms. At 60 ms, stable combustion is achieved. The method of igniting the spark can be summarized as follows: the fuel–air mixture around the igniter is first ignited and thus the flame propagates downward, and the oil-air mixture in the recirculation zone is ignited. And finally, the flame propagates downstream of the combustion chamber until the entire combustion chamber is ignited.

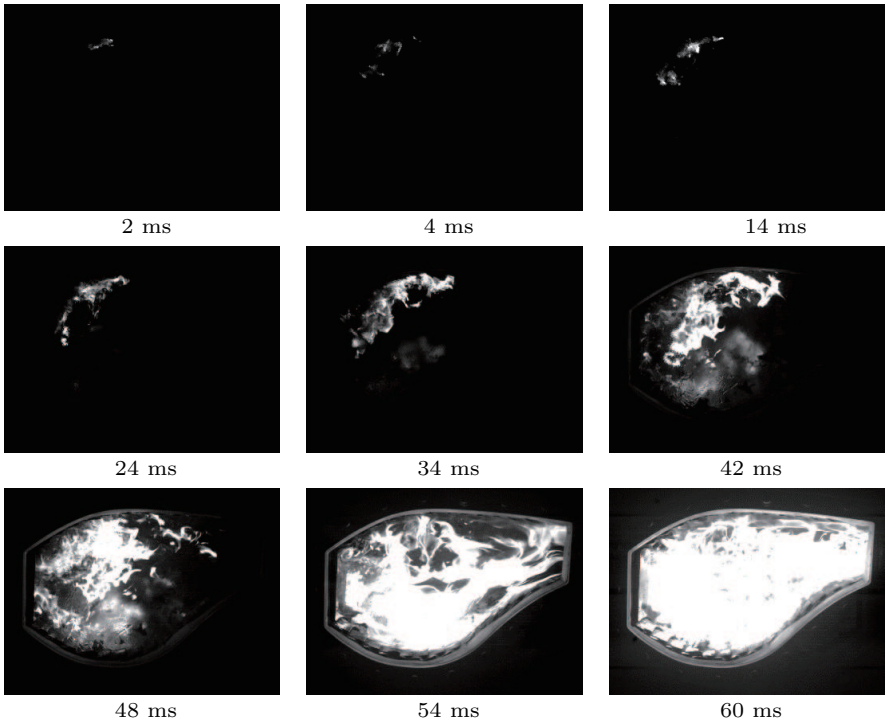


Fig. 11. Ignition process of spark igniter.

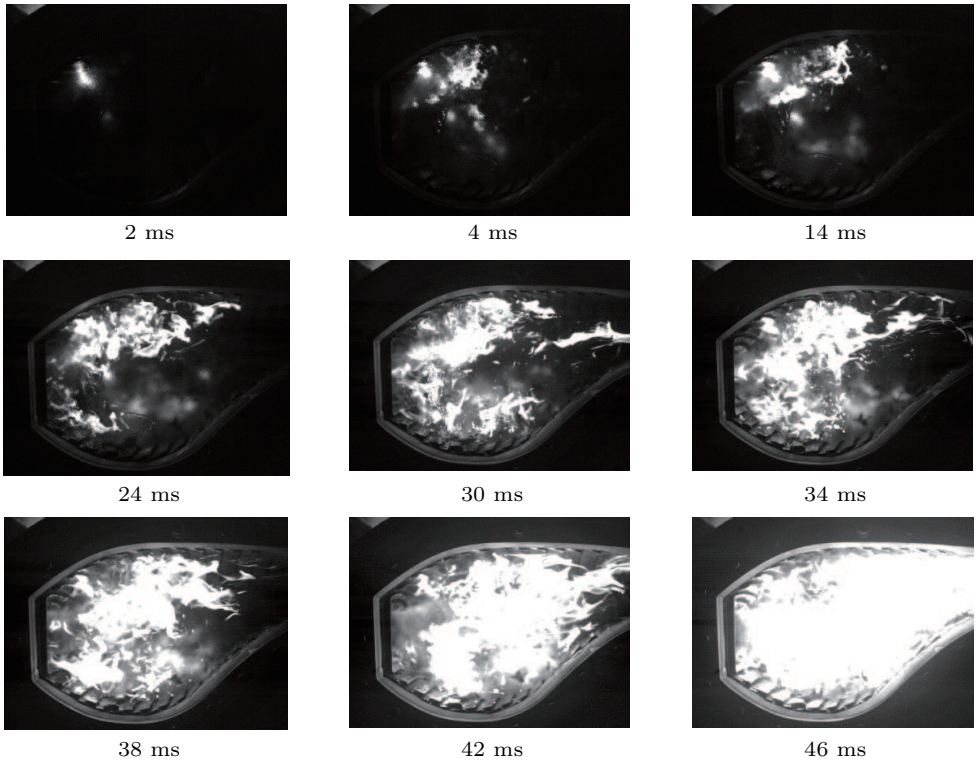


Fig. 12. Ignition process of air plasma jet igniter.

The ignition process of the air plasma jet igniter is shown in Fig. 12. The ignition process of the air plasma jet igniter has an air flow rate of 60 L/min. The discharge result of the air plasma jet igniter corresponding to the ignition process in Fig. 12 is shown in Fig. 13. Comparing Fig. 12 and Fig. 13, it can be found that the igniter breaks down at time 0, forming an arc. In the whole ignition process from 0 to 46 ms, the air plasma jet igniter experiences 4 repeated breakdowns. At 2 ms, the air plasma jet is formed. And then the fuel–air mixture around the air plasma jet region is gradually ignited. Due to the long length of the air plasma jet and the high-temperature, the fuel–air mixture passing through the air plasma jet is preferentially ignited in the upper part of the combustion chamber under aerodynamic forces. At 4 ms, the flame fills the upper half of the combustion chamber. At 4 ms, the flame fills the upper half of the combustion chamber, but the flame does not yet propagate to the lower part of the combustion chamber. At 24 ms, the flame propagates through the upper part of the combustion chamber. And the flame propagates to the bottom of the combustion chamber and begins to propagate downstream of the combustion chamber. At 42 ms, the flame propagates almost to the entire combustion chamber. At 46 ms, it enters into the steady combustion stage.

The fuel–air mixture is ignited after passing through the high-temperature plasma jet. Under the action of the jet aerodynamic force, the jet flame can also quickly reach the recirculation zone and ignite the recirculation zone. But under the influence of the flow field, the lateral propagation speed is much greater than the longitudinal propagation speed. Therefore, the ignition process of the air plasma jet igniter shows the characteristics that the velocity of flame propagation in the upper combustion chamber is different from that in the lower combustion chamber.

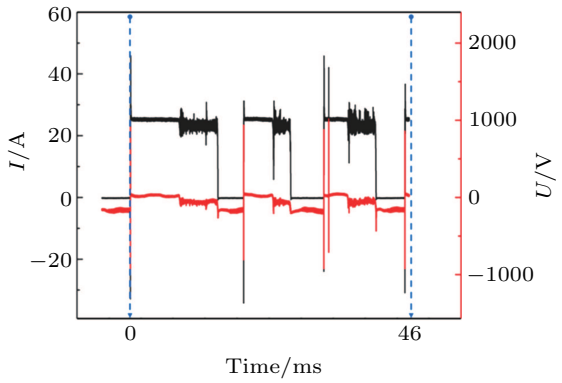


Fig. 13. Discharge characteristics of air plasma jet igniter during ignition.

Figure 14 shows the ignition process of a pre-combustion plasma jet igniter. To keep the jet flow rate of the igniter uniform, the flow rate of methane is 4 L/min, and the air flow rate is 56 L/min. The discharge result of the pre-combustion plasma jet igniter corresponding to the ignition process in Fig. 14 is shown in Fig. 15. The discharge medium is broken down at time 0. It can be seen from Fig. 15 that the arc is always in the stable arc stage after the breakdown. At 2 ms, the pre-combustion plasma jet forms at the exit of the igniter. And a complete jet forms at 3 ms. At 8 ms, it begins to ignite

the fuel–air mixture around the jet. At 15 ms, the upper portion of the entire combustion chamber is substantially ignited. At 34 ms, the flame has almost filled the entire combustion chamber. It enters into a stable combustion stage at 37 ms.

The ignition process of the pre-combustion plasma jet igniter is similar to the ignition process of the air plasma jet igniter, and they have similar characteristics. However, the pre-combustion plasma jet is a kind of high-temperature jet mixed with flame and arc. So it has a longer tongue and a higher initial ignition temperature. It has a stronger penetrating force, which can quickly ignite the recirculation zone. In the process of pre-combustion of methane, The chemical reaction path of the methane self-ignition chemical kinetic process is $CH_4 \rightarrow CH_3 \rightarrow CH_2O \rightarrow CHO \rightarrow CO \rightarrow CO_2$.[22] The free radicals and excited-state particles generated in the discharge process greatly increase the molar concentration of the reactant and increase the reaction rate of chemical equilibrium. It changes the reaction path of methane self-combustion which promotes the reaction.

Comparing Fig. 12 and Fig. 14, it can be found that the flame propagation process and speed are relatively close in the upper part of the combustion chamber. At 15 ms, the pre-combustion plasma jet igniter ignites all of the recirculation zones. But at 24 ms, the air plasma jet just starts to ignite the recirculation zone. It can be found that the pre-combustion plasma jet igniter can ignite the fuel–air mixture in the recirculation zone more quickly in the ignition process. So the flame can propagate down along the longitudinal direction of the combustion chamber earlier, which accelerates the entire ignition process.

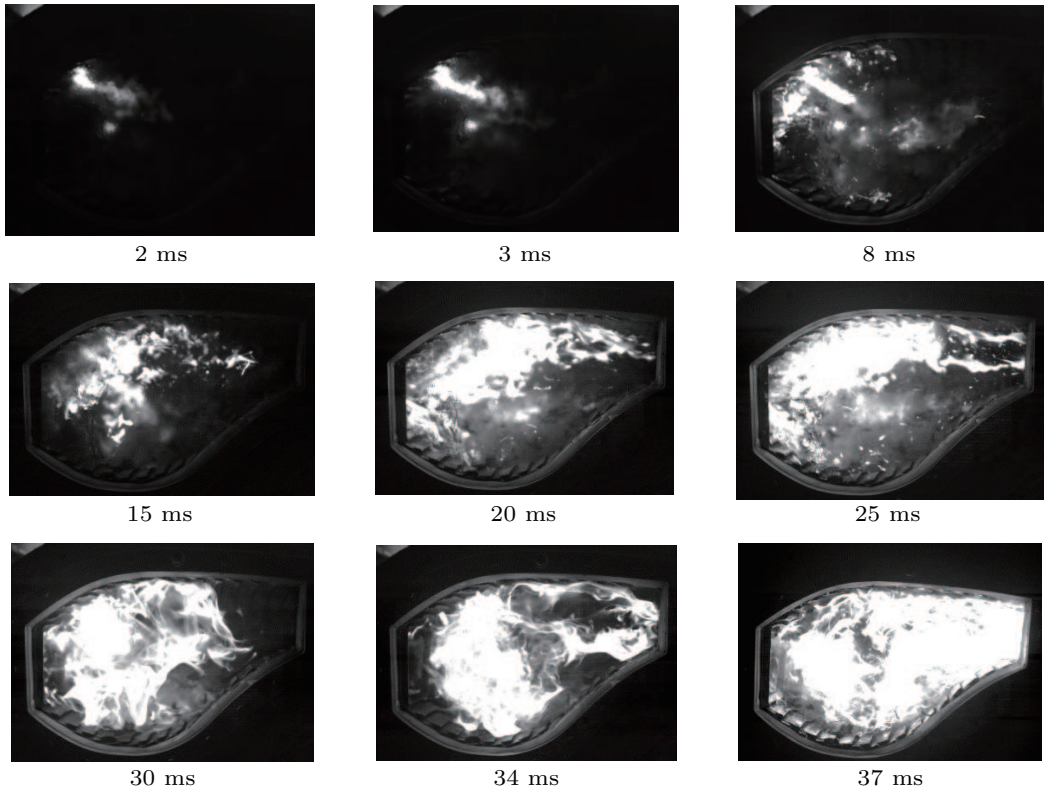


Fig. 14. Ignition process of pre-combustion plasma jet igniter.

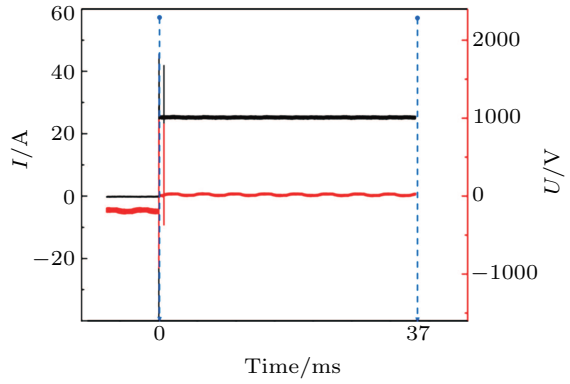


Fig. 15. Discharge characteristics of pre-combustion plasma jet igniter during ignition.

3.3.2. Analysis of ignition delay time

The ignition delay time is an important parameter for studying the ignition process of the igniter. Since combustion is a complex process, currently, no established standard to define the ignition delay time is existent. The photomultiplier has the characteristics of fast response speed and high sensitivity, so the photomultiplier can accurately measure the ignition delay time. During discharge, ionized air can produce a large number of O atoms, and CH is typical intermediate in the combustion process. In this paper, the ignition delay time is defined as the period from the start of the igniter to

the complete ignition of the combustion chamber. Therefore, two photomultipliers are used in the experiment to capture the emission spectrum signals of O (777 nm) and CH (431.4 nm) during ignition. The two photomultipliers are installed on the side of the observation window of the combustion chamber. As shown in area A and area B in Fig. 4, one photomultiplier that captures O (777 nm) is placed at the exit of the igniter, and another photomultiplier that captures CH (431.4 nm) is located at the end of the combustion chamber. Using a narrow band interference filter, the wave plate for filtering the spectrum outside the O (777 nm) atomic emission spectrum is a filter with a center wavelength of 780 nm and a half bandwidth of 5 nm, and the wave plate used to filter the spectrum outside the CH-based (431.4 nm) emission spectrum is a filter with a center wavelength of 430 nm and a half bandwidth of 5 nm.

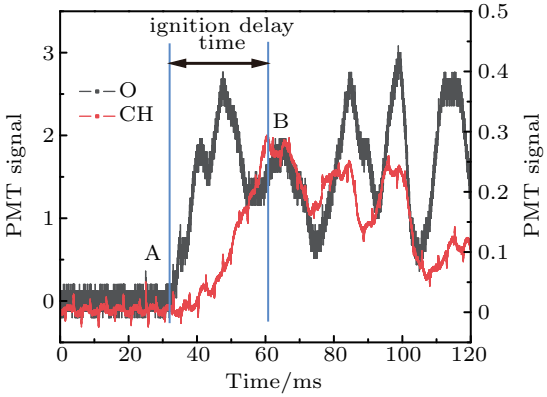


Fig. 16. Schematic diagram of ignition delay time.

Figure 16 shows the schematic diagram of ignition delay time. The intensity of the O (777 nm) emission spectrum at point A begins to increase, indicating that the igniter begins to work. At point B, the emission intensity of the CH (431.4 nm) spectral signal reaches a maximum value, indicating that the ignition process is completed. The time between point A and point B is the ignition delay time.

Figure 17 shows the ignition delay times of different types of igniters at different inlet air temperatures. As can be seen from the figure, the ignition delay time of the pre-combustion plasma jet igniter is significantly less than those of the other two igniters. As explained in Subsubsection 3.3.1, this is mainly because the ignition modes of the three igniters are different, resulting in a difference in the ignition delay time. The pre-combustion plasma jet igniter has a methane pre-combustion process. So it has a longer ignition jet and a higher jet temperature, which greatly improves its ignition capacity and shortens the ignition delay time. When the airflow at the inlet of the combustion chamber is 300 m^3/h, 400 m^3/h, and 500 m^3/h, respectively, that is, the inlet air velocity is 23.47 m/s, 31.29 m/s, and 39.11 m/s, as the speed increases, the ignition delay time decreases. This is because the airflow velocity is increased, which increases the turbulence of the flow field in the combustion chamber, thus causing the flame front to split into more combustion centers, resulting in a great increase of turbulent flame propagation speed. At the same time, the small-scale turbulence from the mixing holes of the combustion chamber will greatly increase the degree of blending the flame surface molecules with the molecules in the fresh air, so the turbulent flame propagation speed increases.

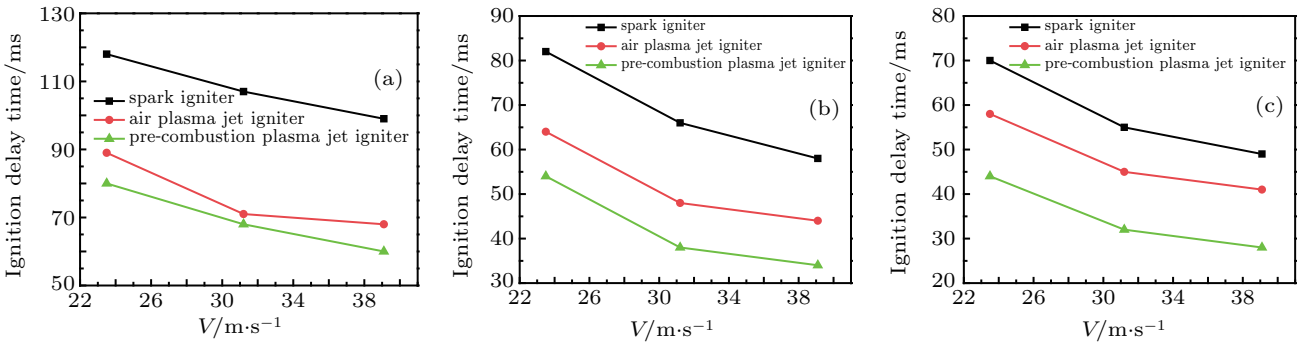


Fig. 17. Ignition delay times of different types of igniters: (a) 60 °C, (b) 80 °C, and (c) 100 °C.

Besides, as can be seen by comparing Figs. 15(a), 15(b), and 15(c), as the inlet airflow temperature is increased, the ignition delay times of the three igniters are gradually shortened. When the inlet air temperature is 60 °C and the inlet airflow velocity is 39.11 m/s, the ignition delay time of the pre-combustion plasma jet igniter is 60 ms, the ignition delay time of the air plasma jet igniter is 68 ms, and the ignition delay time of the spark ignition igniter is 99 ms. The ignition delay time of the pre-combustion plasma jet igniter is 39.4% shorter than that of the spark igniter, and 11.2% shorter than that of the air plasma jet igniter. When the inlet airflow temperature is 100 °C and the inlet airflow velocity is 39.11 m/s, the ignition delay time of the pre-combustion plasma jet igniter is 28 ms, the ignition delay time of the air plasma jet igniter is 41 ms, and the ignition delay time of spark igniter is 49 ms. The pre-combustion plasma jet igniter ignition delay time is 22.4% shorter than the ignition delay time of the spark igniter and 7.3% shorter than that of air plasma jet ig-

niter. which are 11 s and 3 s. As the inlet air temperature increases, the difference between the ignition delay times of the three igniters gradually decreases. The advantages of the pre-combustion plasma jet igniter are even more pronounced when the inlet airflow temperature is low. Therefore, when the aircraft is turned off under high-altitude and low-temperature conditions, the pre-combustion plasma jet igniter has a more obvious advantage in the ignition.

3.3.3. Analysis of ignition boundary

Ignition boundary here refers to the concentration limit of mixed gas which can be ignited under certain conditions. The ignition boundary directly determines the reliable working range of aero-engine and is one of the most important parameters to characterize the igniter performance.

In this paper, the ignition boundary of pre-combustion plasma jet igniter, air plasma jet igniter and spark igniter are studied on condition that the inlet air temperature is 80 °C. As shown in Fig. 18, taking the inlet air velocity as the horizontal coordinate and the residual air coefficient as the vertical coordinate, the poor ignition boundary of the igniter is obtained. The calculation formula of the excess coefficient is

$$\alpha = \frac{W_{\mathrm{a}}}{W_{\mathrm{f}} \cdot L}. \tag{1}$$

In the formula, W_{a} is the air flow involved in combustion, W_{f} is the fuel inflow, L_0 is the theoretical amount of air, which is the theoretical amount of air required for the complete combustion of 1-kg fuel. When aviation kerosene is used as fuel, $L_0 = 14.7$ for the combustion chamber.

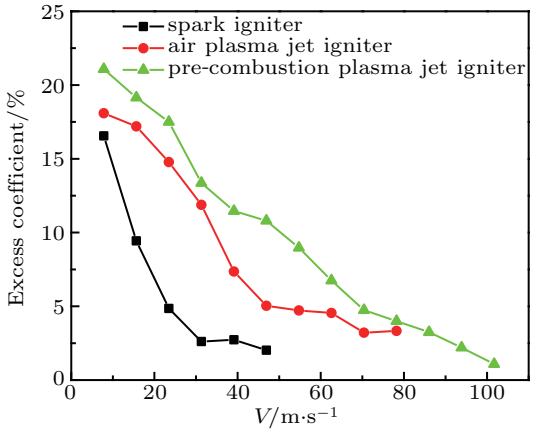


Fig. 18. Ignition boundaries for three different igniters.

It can be seen from Fig. 18 that the trends of lean ignition boundary of three different igniters are the same. That is, with the increase of the inlet airflow velocity in the combustion chamber, the range of the excess coefficient is gradually reduced. The maximum airflow speed at which the spark igniter can be ignited is 46.94 m/s. The maximum airflow speed at which the air plasma jet igniter can be ignited is 78.23 m/s, and the maximum speed at which the pre-combustion plasma jet igniter can be ignited is 101.69 m/s. The maximum speed of the ignition boundary of the pre-combustion plasma jet igniter is 2.2 times that of the spark igniter and 1.3 times that of the air plasma jet igniter.

When the inlet air flow is 100 m^3/h ($v = 7.82$ m/s), the maximum excess coefficient that can be ignited by the spark igniter is 16.5, and the maximum excess coefficient at which the air plasma jet igniter can be ignited is 18.09. The maximum excess coefficient at which the pre-combustion plasma jet igniter is ignitable, is 21.08. The ignition boundary of the pre-combustion plasma jet is 27.4% larger than that of the spark igniter, and it is 16.5% larger than that of the plasma jet igniter. When the inlet airflow velocity is 500 m^3/h ($v = 39.11$ m/s), the ignition boundary of the pre-combustion plasma jet igniter is expanded by 319.8% compared with the spark igniter. The ignition boundary is expanded by 55.7% compared with the air plasma jet igniter. It can be seen that as the airflow speed increases, the ignition advantage of the pre-combustion plasma jet igniter is more obvious.

4. Conclusions

In this paper, the discharge characteristics, jet characteristics and ignition characteristics of the pre-combustion plasma jet igniter are studied. The conclusions drawn from the present study are as follows.

(I) As the equivalent ratio of the jet gas increases, the average arc stability time and duty cycle increase. This is mainly due to the fact that as equivalent ratio increases, a large number of active particles produced by the combustion of methane are more favorable for the formation of discharge channels, which make the arc not easily blown off by the jet gas.

(II) Besides, the working power also gradually decreases as equivalent ratio increases. Because the energy required to break C–H in methane molecule is less than that needed to break O=O in the O_2 molecule and N≡N in the N_2 molecule. With the increase of the jet gas equivalent ratio of the igniter, the jet length and the core area of the jet gradually increase. Methane combustion is also conducive to the formation of the discharge path, so the working power is reduced.

(III) The ignition process of pre-combustion plasma jet igniter is different from that of spark igniter and air plasma jet igniter. It has a longer plasma jet and it can ignite the fuel–air mixture in the recirculation zone more quickly, thus speeding up the ignition process.

(IV) The ignition performance of the pre-combustion plasma jet igniter is significantly better than that of the air plasma jet igniter and the spark igniter. It can shorten the ignition delay time and significantly expand the ignition boundary. When the flow rate of inlet air is 500 m^3/h, that is, the inlet air velocity is 39.11 m/s, the ignition boundary of the pre-combustion plasma jet igniter is 319.8% larger than that of the

spark igniter, and is 55.7% larger than the ignition boundary of the air plasma jet igniter.

References

[1] Cheng Y F, Ni W S and Li G Q 2012 *Acta Phys. Sin.* **61** 060509 (in Chinese)
[2] Tang W H, Xu B B, Ran X W and Xu Z H 2017 *Acta Phys. Sin.* **66** 030505 (in Chinese)
[3] Zhang P, Zhong W L, Li Q, Yang B, Li Z G and L X 2017 *Chin. Phys. B* **26** 110501
[4] Yu J L, He L M, Ding W, Cheng Y G and Wang J J 2015 *J. Combust. Sci. Technol.* **2015** 511
[5] Tang M X, Wu Y, Wang H Y, Guo S K, Sun Z Z and Sheng J M 2018 *Exp. Therm. Fluid Sci.* **99** 584
[6] Du H L, He L M, Lan Y D and Wang F 2011 *J. Air Force Eng. University (Nat. Sci. Ed.)* **12** 11
[7] Guo X Y, He L M, Lan Y D and Chen D 2008 *J. Projectiles Rockets Missiles Guidance* **30** 307
[8] He L M, Qi W T, Zhao B B, Chen G C, Bai X F and Duan K L 2015 *High Voltage Eng.* **41** 2030
[9] Lan Y D, He L M and Ding W 2010 *High Voltage Apparatus* **46** 35
[10] Huang D Q, Yu J L, Wang S B, Li Q Y and He L M 2018 *High Voltage Eng.* **44** 3068
[11] Ju Y G, Joseph K L, Reuter C B, Won S H, Yang X L, Yang S, Sun W T, Jiang Z L and Chen Q 2016 *Plasma Chem. Plasma Process.* **36** 85
[12] Ju Y G and Sun W T 2015 *Prog. Energy Combust. Sci.* **48** 21
[13] Mao X Q, Rousso A, Chen Q and Ju Y G 2019 *Proc. Combust. Inst.* **37** 5545
[14] Dresevn S V and Cheron T 1972 *Physics and technology of low-temperature plasma* (Moscow: Atomic Energy Press)
[15] Pfender E, Fincke J and Spores R 1991 *Plasma Chem. Plasma Process.* **11** 529
[16] Pfender E 1999 *Plasma Chem. Plasma Process.* **19** 1
[17] Bozhenkov S A, Starikovskaya S M and Starikovskii A Y 2003 *Combust. Flame* **133** 133
[18] Yu J L, He L M, Hu Z, Zhang Q, Xiao Y, Jiang Y J and Wu Y 2018 *Proc. Inst. Mech. Eng. Part. G* **232** 1685
[19] Yu J L, He L M, Ding W, Zhao Z C and Zhang H L 2016 *Appl. Therm. Eng.* **98** 265
[20] Watanabe H, Takegahara H and Aoyagi J 2017 *J. Propul. Power* **2017** 1
[21] Wang F, He L M, Cao N C, Lan Y D, Wang J X, Wang y and Du H L 2010 *High Voltage Eng.* **36** 2537
[22] Kosarev I N, Aleksandrov N L, Kindysheva S V, Starikovskaia S M and Starikovskii A Y 2009 *Combust. Flame* **156** 221
[23] Wang S B, Yu J L, Cheng W D, Ma Y, Zheng R Z, Huang D Q and He L M 2019 *Chem. Phys. Lett.* **730** 399